Escola de Primavera de Transição e Turbulência
Blumenau 2020

ABCM Associação Brasileira de Engenharia e Ciências Mecânicas

12th Spring School on Transition and Turbulence
September 21st-25th, 2020, Blumenau, SC, Brazil

EPTT-2020-0047
HYDRODYNAMIC STABILITY ANALYSIS IN HIGH WEISSENBERG NUMBER FLOWS VIA LOG-CONFORMATION TRANSFORMATION

Beatriz Liara Carreira
Analice Costacurta Brandi
Faculdade de Ciências e Tecnologia, Universidade Estadual Paulista "Júlio de Mesquita Filho"
liara.carreira@unesp.br; analice.brandi@unesp.br

Matheus Tozo de Araujo
Laison Junio da Silva Furlan
Leandro Franco de Souza
Instituto de Ciências Matemáticas e de Computação, Universidade de São Paulo
matheustozo@gmail.com, laisonfurlan@usp.br, lefraso@icmc.usp.br

Abstract. *Over time, several authors have dedicated themselves to investigating the causes and developing stabilizing methods for a difficulty that became known as the High Weissenberg Number Problem (HWNP), which consists in numerical instabilities arising from the collapse of numerical schemes applied in the constitutive equation solution for non-Newtonian fluids. The log-conformation formulation has highlight in the literature and consists of the application of the logarithmic transformation to the conformation tensor. Therefore, the aim of the present work is to use the log-conformation method as code stabilizing technique to investigate the hydrodynamic stability of the two-dimensional Poiseuille flow for Giesekus fluid by means of Direct Numerical Simulation (DNS) considering high Weissenberg numbers.*

Keywords: *high Weissenberg number problem, log-conformation method, Direct Numerical Simulation, Poiseuille flow.*

1. INTRODUCTION

The Computational Fluid Dynamics – area of scientific computation that studies computational methods for simulating phenomena involving motion of fluids – is increasingly used as a tool for modeling and simulating flows that are of interest in industry. Among the industrial applications is the treatment of non-Newtonian fluid flows. Increasingly, polymers are replacing other materials, therefore, it is essential that the polymeric product presents a satisfactory mechanical performance during the projected useful life for a given application. One of the main characteristics of polymers is viscoelasticity, which consists of the presence of viscous and elastic properties at the same time. Various materials used in industrial applications such as in oil industries, paints and in cosmetic products, behave like viscoelastic fluids.

Laminar flows are always subject to small disturbances that can occur due to several factors, such as structural vibration, surface roughness, noise, external turbulence, among others. If these disturbances are not dampened, the laminar flow undergoes a transition to another more complex state, but not necessarily a state turbulent (Souza *et al.*, 2005). This process, known as laminar-turbulent transition, is extremely complex and is not completely understood, mainly for non-Newtonian fluid flows. The analysis of hydrodynamic stability is performed with the objective of forecast changes that occur in the flow of a fluid in laminar regime and that are potentially capable to lead it to the turbulent regime, and the mechanisms of hydrodynamic instability have an important role in this transition process.

One of the dimensionless parameters that characterize the flow of viscoelastic fluids is the Weissenberg number, which is the ratio between the elastic relaxation time and the time associated with the local deformation of the fluid time. However, an difficult usually found in the simulation of viscoelastic flows, consists in the loss of convergence from a critical value of the Weissenberg number. This limitation became known as the High Weissenberg Number Problem (HWNP). Although little understood, one of the causes of HWNP from a numerical point of view, is related to the loss of positivity of the tensors. According to Dupret and Marchal (1986), the evolutionary character of a system is a requirement that must be maintained, regardless of the model considered.

An approach that emerged in the attempt to solve the HWNP formulates the model from the conformation tensor due to its properties of being symmetrical and positive defined (Hulsen, 1988). The main technique for the solution of the HWNP in Computational Rheology, known as log-conformation, was presented by Fattal and Kupferman (2004, 2005) and consists of reformulate the constitutive laws that describe the non-Newtonian behavior in terms of the logarithm of the conformation tensor.

In this sense, the objective of this work is to present the log-conformation technique for HWNP stabilization. Considering the two-dimensional Poiseuille flow of Giesekus viscoelastic fluid, the stability analysis for flows will be performed using the Direct Numerical Simulation (DNS) technique and a numerical study of the log-conformation formulation (Fattal and Kupferman, 2004) was carried out in order to demonstrate the relevance of this methodology in the solution of simulated flows with a high Weissenberg number.

2. MATHEMATICAL FORMULATION

The flow is assumed to be unsteady, non-Newtonian, two-dimensional and incompressible, without body forces. The conservation of mass (continuity) and conservation of momentum equations governing the flow, in the dimensionless form, are given by

$$\nabla \cdot \mathbf{u} = 0, \tag{1}$$

$$\frac{\partial \mathbf{u}}{\partial t} + \nabla \cdot (\mathbf{uu}) = -\nabla p + \frac{\beta}{Re}\nabla^2 \mathbf{u} + \nabla \cdot \mathbf{T}, \tag{2}$$

where **u** denotes the velocity field, t is the time, p is the pressure and **T** is the non-Newtonian extra-stress tensor (symmetric), given by $\mathbf{T} = \begin{bmatrix} T^{xx} & T^{xy} \\ T^{xy} & T^{yy} \end{bmatrix}$.

The dimensionless parameter $Re = \rho UL/\eta_0$ is associated with the Reynolds number, where L and U denote length and velocity scales respectively, and ρ is the fluid density. The amount of Newtonian solvent is controlled by the dimensionless solvent viscosity coefficient $\beta = \eta_s/\eta_0$, where $\eta_0 = \eta_s + \eta_p$ denotes the total shear viscosity, being η_s and η_p the Newtonian solvent and polymeric viscosities, respectively.

In this paper we worked with viscoelastic fluid flow governed by the non-linear Giesekus constitutive equation (Giesekus, 1982), that is given by

$$\mathbf{T} + Wi\overset{\triangledown}{\mathbf{T}} + \alpha_G \frac{WiRe}{1-\beta}(\mathbf{T}\cdot\mathbf{T}) = \frac{1-\beta}{Re}(\nabla\mathbf{u} + \nabla\mathbf{u}^\top), \tag{3}$$

where α_G is the mobility parameter that regulates the shear thinning behavior of the fluid ($0 \leq \alpha_G \leq 1$), $\mathbf{T}\cdot\mathbf{T}$ is a tensor product and $\overset{\triangledown}{\mathbf{T}}$ is the upper-convected derivative. The dimenssionless parameter $Wi = \lambda U/L$ is called Weissenberg number, being λ the relaxation-time of the fluid.

2.1 Log-Conformation Transformation

An alternative way to describe viscoelastic models uses the tensor conformation **A**. This tensor is symmetric and positive definite and its constitutive equation can be written as (Martins *et al.*, 2015)

$$\frac{\partial \mathbf{A}}{\partial t} + \nabla \cdot (\mathbf{uA}) = \nabla\mathbf{u}\mathbf{A} + \mathbf{A}\nabla\mathbf{u}^\top + \frac{1}{Wi} f(\mathbf{A})P(\mathbf{A}), \tag{4}$$

being the ratio between the extra-stress tensor **T** and **A** given by $\mathbf{T} = \xi(\mathbf{A} - \mathbf{I})$, where ξ is a scalar defined as $\xi = (1-\beta)/ReWi$.

The scalar function $f(\mathbf{A})$ and the tensor $P(\mathbf{A})$, that depends of **A**, are defined according to the model used. In particular, for the Giesekus model $f(\mathbf{A}) = 1$ and $P(\mathbf{A}) = (\mathbf{I} - \mathbf{A})[\mathbf{I} + \alpha_G(\mathbf{A} - \mathbf{I})]$.

Defining $\mathbf{\Psi} = ln(\mathbf{A})$ as the logarithm of the tensor conformation **A**, then $e^{\mathbf{\Psi}} = \mathbf{A}$. After all the algebraic manipulations involved in the construction of the method, an evolution equation for the logarithmic transformation applied to the conformation tensor is finally obtained

$$\frac{\partial \mathbf{\Psi}}{\partial t} + \nabla \cdot (\mathbf{u\Psi}) = (\Omega\mathbf{\Psi} - \mathbf{\Psi}\Omega) + 2\mathbf{B} + \frac{f(e^{\mathbf{\Psi}})}{Wi} e^{-\mathbf{\Psi}} P(e^{\mathbf{\Psi}}), \tag{5}$$

where the tensor **B**, which commutes with **A** (Afonso *et al.*, 2012), arises from a reformulation of the velocity gradient and its transpose, performed by Fattal and Kupferman (2005).

3. DIRECT NUMERICAL SIMULATION

In order to simplify the problem and eliminate the pressure treatment in the momentum equations, we chose the vorticity-velocity formulation (Brandi *et al.*, 2017). Then, the two-dimensional vorticity ω_z is defined by

$$\omega_z = \frac{\partial u}{\partial y} - \frac{\partial v}{\partial x}. \tag{6}$$

Applying such formulation, therefore, the problem is to solve the system composed by Eqs. (7) – (12),

$$\frac{\partial u}{\partial x} + \frac{\partial v}{\partial y} = 0, \tag{7}$$

$$\frac{\partial^2 v}{\partial x^2} + \frac{\partial^2 v}{\partial y^2} = \frac{\partial \omega_z}{\partial x}, \tag{8}$$

$$\frac{\partial \omega_z}{\partial t} + \frac{\partial \omega_z}{\partial x}u + \frac{\partial \omega_z}{\partial y}v = \frac{\beta}{Re}\left[\frac{\partial^2 \omega_z}{\partial x^2} + \frac{\partial^2 \omega_z}{\partial y^2}\right] - \frac{\partial^2 T^{xy}}{\partial x^2} - \frac{\partial^2 T^{yy}}{\partial x \partial y} + \frac{\partial^2 T^{xx}}{\partial y \partial x} + \frac{\partial^2 T^{xy}}{\partial y^2}, \tag{9}$$

$$T^{xx} + Wi\left(\frac{\partial T^{xx}}{\partial t} + \frac{u\partial T^{xx}}{\partial x} + \frac{v\partial T^{xx}}{\partial y} - 2T^{xx}\frac{\partial u}{\partial x} - 2T^{xy}\frac{\partial u}{\partial y}\right) + \alpha_G \frac{WiRe}{1-\beta}\left(T^{xx^2} + T^{xy^2}\right) = 2\frac{1-\beta}{Re}\frac{\partial u}{\partial x}, \tag{10}$$

$$T^{xy} + Wi\left(\frac{\partial T^{xy}}{\partial t} + \frac{u\partial T^{xy}}{\partial x} + \frac{v\partial T^{xy}}{\partial y} - T^{xx}\frac{\partial v}{\partial x} - T^{yy}\frac{\partial u}{\partial y}\right) + \alpha_G \frac{WiRe}{1-\beta}\left(T^{xy}\left(T^{xx} + T^{yy}\right)\right) = \frac{1-\beta}{Re}\left(\frac{\partial v}{\partial x} + \frac{\partial u}{\partial y}\right), \tag{11}$$

$$T^{yy} + Wi\left(\frac{\partial T^{yy}}{\partial t} + \frac{u\partial T^{yy}}{\partial x} + \frac{v\partial T^{yy}}{\partial y} - 2T^{xy}\frac{\partial v}{\partial x} - 2T^{yy}\frac{\partial v}{\partial y}\right) + \alpha_G \frac{WiRe}{1-\beta}\left(T^{xy^2} + T^{yy^2}\right) = 2\frac{1-\beta}{Re}\frac{\partial v}{\partial y}, \tag{12}$$

where Eq. (8) is the Poisson equation for the v velocity component, obtained deriving Eq. (6) with respect to x. Equation (9) is obtained deriving the momentum equation in direction y with respect to x and subtracting the derivative of the momentum equation in direction x with respect to y.

3.1 Base Flow

In this paper we study viscoelastic plane Poiseuille flow where x and y represent the streamwise and wall-normal directions. To calculate the base flow, it is assumed that all variables are dependent only on the y axis, except for the pressure whose gradient is constant in the x direction. The domain in the y direction is comprised between $[-1, 1]$.

However, considering the Giesekus model, the system of equations that derives from these hypotheses does not have a complete analytical solution available in the literature. Therefore, in this work, the base flow was generated numerically by two-dimensional DNS code, without disturbances, and the simulations performed until the flow reached the steady state. Also, the variables for the base flow were taken in the middle of the channel.

4. NUMERICAL METHOD

The system of Eqs. (7) – (12) is solved numerically in the domain as shown in Fig. 1. The calculations are performed on an orthogonal uniform grid, parallel to the wall. The fluid enters the computational domain at $x = x_0$ and exits at the outflow boundary $x = x_{max}$. In this work, the infinitesimal disturbances behavior in the flow is investigated. Unsteady disturbances are introduced through suction and blowing of mass in the wall in the region between x_1 and x_2. In the initial time $t = 0$ the flow has no disturbances. After an interval, more specifically at time $t + \delta t$, disturbances are inserted in a disturbances trip near the inflow, through the imposition of velocity v:

$$v = Af(x)sin(\omega_t t), \quad x_1 < x < x_2, \tag{13}$$

and

$$v = 0, \quad x \leq x_1 \quad \text{or} \quad x \geq x_2, \tag{14}$$

where A is the parameter used to adjust the disturbance amplitude, $f(x)$ is a 9th-order function, ω_t is a disturbance time frequency and the points x_1 and x_2 are the extreme limits of the strip where the disturbance is introduced.

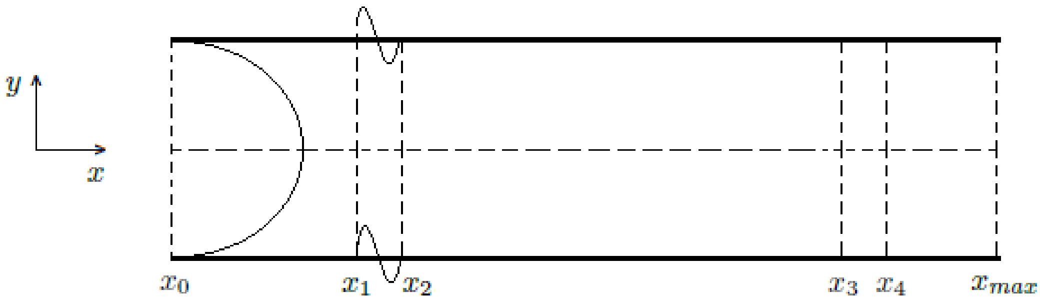

Figure 1: Definition of the computational domain for Poiseuille flow.

In the region located between x_0 and x_1 and x_3 and x_4 a buffer domain technique is implemented in order to avoid wave reflections from the inflow and outflow boundaries, respectively.

In the numerical method the time derivatives in the vorticity transport and the components of the non-Newtonian extra-stress tensor equations are discretized with a classical four step fourth-order Runge-Kutta integration scheme. The spatial derivatives are calculated using a high-order compact finite difference-schemes. The use of the adopted compact finite differences to estimate the first and second spatial derivatives requires the solution of tridiagonal linear systems. The numerical derivative approximations have 5th- and 6th-order of accuracy. The Poisson equation is solved using a multigrid Full Approximation Scheme (FAS).

Finally, with the purpose of eliminating numerical (spurious) oscillations, a filter is applied after the last Runge-Kutta step. This filter is applied in the vorticity component in the streamwise direction and in the non-Newtonian extra-stress tensor components.

We solve the system composed by Eqs. (7) – (12) numerically by the application of the following algorithm:

Step 1: Apply a step of the time integrator for the vorticity and the non-Newtonian extra-stress tensor.

Step 2: Apply the functions responsible for the damping and relaminarization zones.

Step 3: Introduce the suction and injection disturbances into the walls.

Step 4: Calculate the right side of the Poisson equation, given by Eq. (8).

Step 5: Calculate the v velocity by solving the Poisson equation [Eq. (8)].

Step 6: Calculate the value of u velocity through Eq. (7).

Step 7: Calculate the ω_z vorticity through Eq. (9).

Step 8: Calculate the components of the non-Newtonian extra-stress tensor through Eqs. (10) – (12).

Step 9: Update the vorticity value ω_z and the components of the non-Newtonian extra-stress tensor at the walls.

Step 10: Apply the filter after the last sub-step of the time integrator.

The numerical simulation finishes when the desired wall clock time is reached.

5. CODE VERIFICATION

The verification test in this work occurs for a DNS code that simulates the two-dimensional, incompressible and isothermal Poiseuille problem, considering the viscoelastic fluid of the Giesekus model, and the log-conformation formulation as a stabilizing technique for simulations with the high Weissenberg number.

Numerical simulations were performed in order to compare the base flow generated numerically using the DNS technique considering $\alpha_G = 0$ in Eq. (3) that represents the Giesekus model, with the flow analytical solution under the same conditions considering the Oldroyd-B. This is valid, because when $\alpha_G = 0$ the equation of the Giesekus model is reduced to the Oldroyd-B model.

The parameters adopted for numerical simulation of the verification test were: the number of points in the streamwise and wall-normal directions are $i_{max} = 9049$ and $j_{max} = 249$, respectively; the distance between two consecutive points in the x and y directions are $dx = 2\pi/(16\alpha_r)$ and $dy = 2/(j_{max} - 1)$, respectively, where α_r is the real part of the wavenumber; the time steps per wave period are 248.

Figure 2 shows the comparison between the analytical solution of Oldroyd-B fluid and the numerical solution obtained using a DNS technique for Giesekus fluid considering $\alpha_G = 0$. In this figure was performed three simulations, considering $Re = 2000$; 4000 and 7000, $\beta = 0.25$; 0.50 and 0.50, and $Wi = 10$; 15 and 20.

Figure 2 is performed to verify the behavior of T^{xx} and T^{xy} non-Newtonian tensors and it is possible to notice that the behavior both formulations are in agreement.

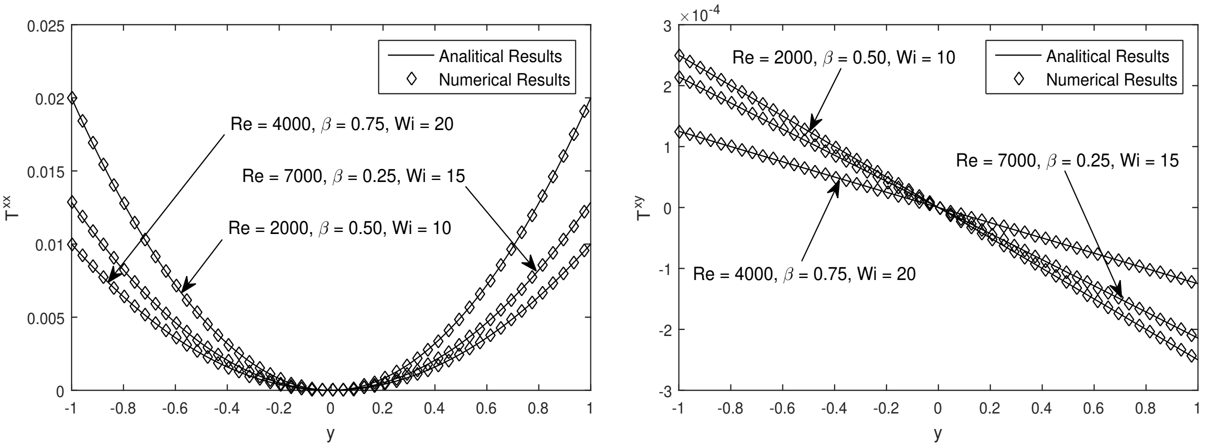

(a) (b)

Figure 2: Numerical solutions obtained at the middle of the channel for Giesekus and Oldroyd-B fluids flows using different parameters.

6. RESULTS

Different numerical simulations are presented to verify the effect that the application of the log-conformation transformation produces as a HWNP stabilizing technique in a Poiseuille flow considering the Giesekus viscoelastic fluid. Variations of the constant β are considered ($\beta = 0.25$; 0.50 and 0.75) in comparison with the Newtonian fluid, for $Re = 2000$, $\alpha_G = 0.15$ (Fig. 3); 0.30 (Fig. 4) and 0.45 (Fig. 5) and variations of Wi, such as $Wi = 5$; 20; 80 and 120.

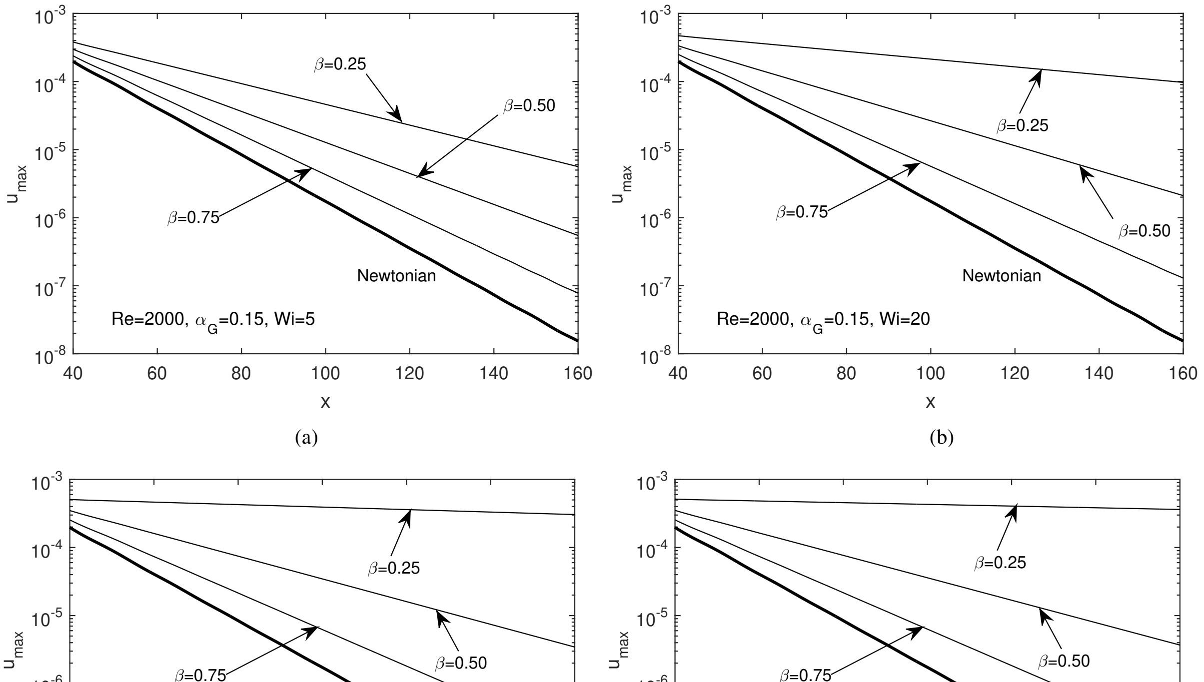

(a) (b)

(c) (d)

Figure 3: Maximum streamwise velocity disturbance development in the streamwise direction for different β values, considering $Re = 2000$, $\alpha_G = 0.15$ and: (a) $Wi = 5$; (b) $Wi = 20$; (c) $Wi = 80$ and (d) $Wi = 120$.

The parameters adopted in DNS simulations carried out here were: the number of points in the streamwise and wall-normal directions are $i_{max} = 505$ and $j_{max} = 249$, respectively; the distance between two consecutive points in the x and y-directions are $dx = 2\pi/(16\alpha_r)$ and $dy = 2/(j_{max} - 1)$, where α_r is the real part of the wavenumber. Also, was adopted 128 time steps per wave period, disturbance frequency $\omega_t = 0.2$ and the parameter A to adjust the amplitude of the Tollmien-Schlichting waves was 1×10^{-4}.

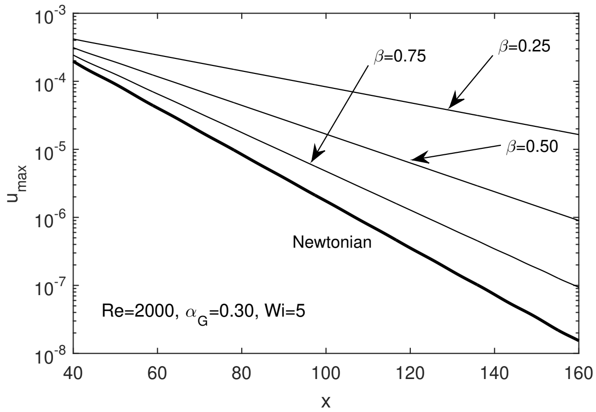

(a)

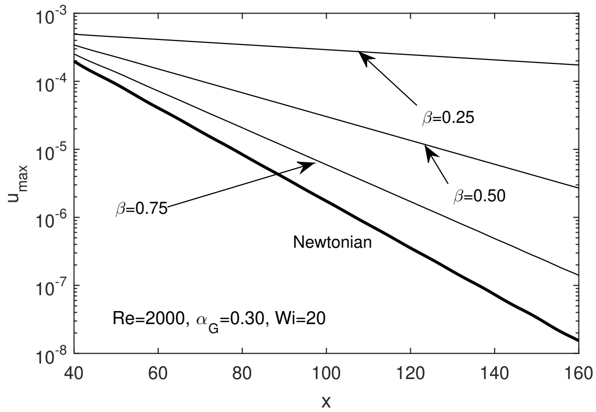

(b)

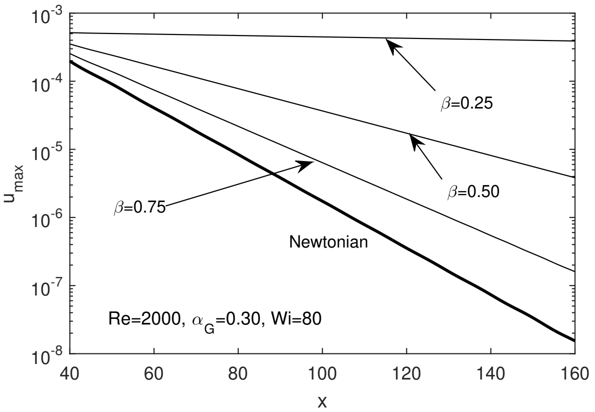

(c)

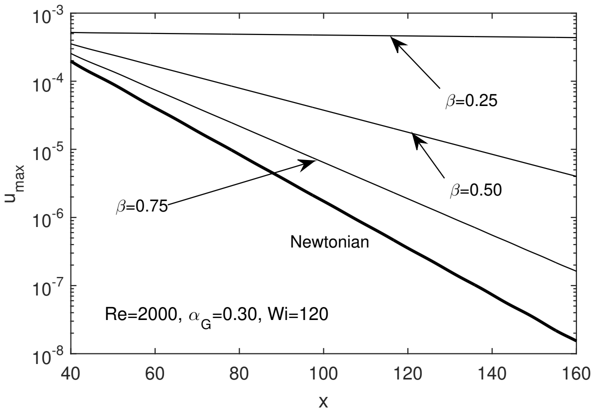

(d)

Figure 4: Maximum streamwise velocity disturbance development in the streamwise direction for different β values, considering $Re = 2000$, $\alpha_G = 0.30$ and: (a) $Wi = 5$; (b) $Wi = 20$; (c) $Wi = 80$ and (d) $Wi = 120$.

Note that for higher Weissenberg numbers, the curves become less decreasing. This effect is more visible when β is lower, that is, when there is a fluid more distant from the Newtonian fluid. In these cases, in particular, for $\beta = 0.25$, increases in Wi numbers cause loss of flow stability, generating neutral cases (Fig. 3(c), 3(d), 4(c), 4(d), 5(c), 5(d)). In

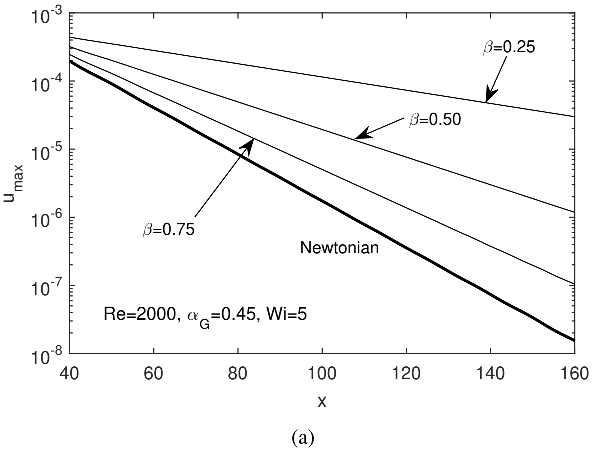

(a)

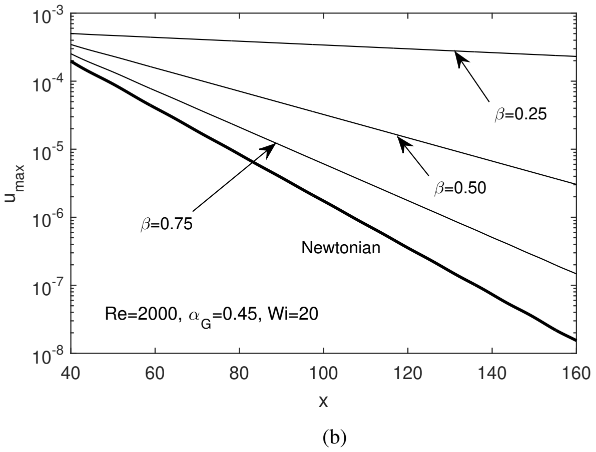

(b)

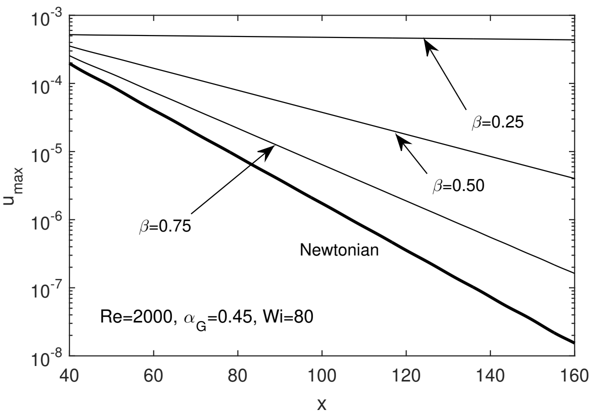

(c)

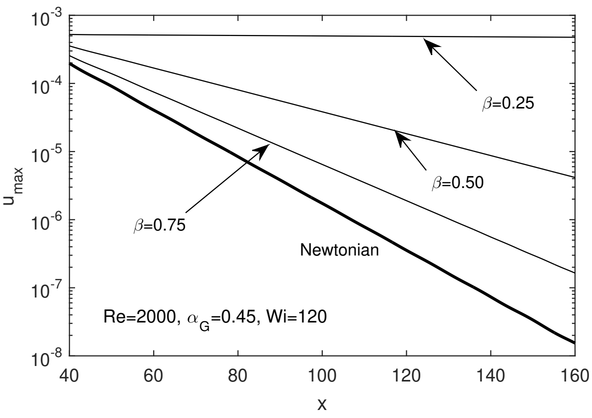

(d)

Figure 5: Maximum streamwise velocity disturbance development in the streamwise direction for different β values, considering $Re = 2000$, $\alpha_G = 0.45$ and: (a) $Wi = 5$; (b) $Wi = 20$; (c) $Wi = 80$ and (d) $Wi = 120$.

contrast, the most stable cases are noticed when $\beta = 0.75$.

In addition, it can see that the parameter α_G also influences the flow stability, because as its value decreases, more stable flows are obtained, i.e., the disturbances are more dampened. This can be seen best when the Wi number is smaller. Also, among the simulated cases, non-Newtonian fluids are always less stable than Newtonian fluids, although instability has not occurred. In addition, for the lowest β values, as Weissenberg numbers increases, the flow becomes less stable.

The positivity of the conformation tensor is a characteristic that must be preserved throughout the time evolution of the

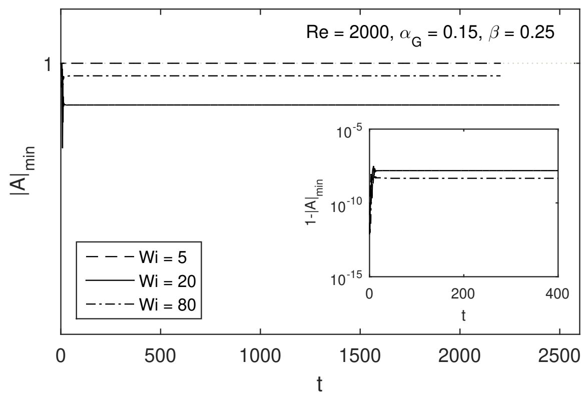

(a)

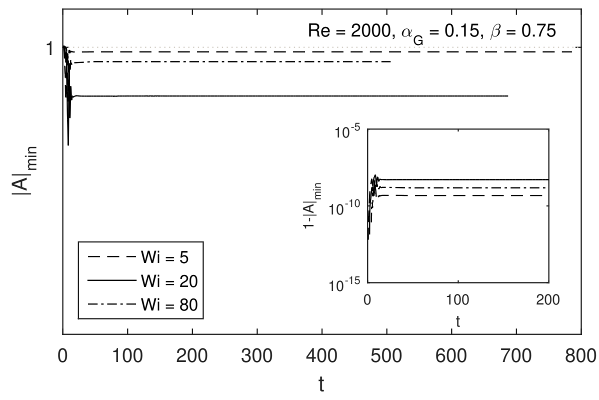

(b)

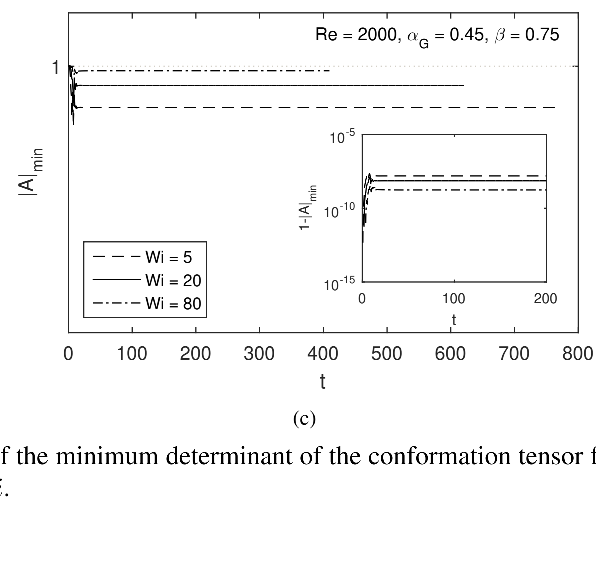

(c)

Figure 6: Temporal evolution of the minimum determinant of the conformation tensor for $Re = 2000$, $\alpha_G = 0.15$; 0.45, $\beta = 0.25$; 0.75 and varying Wi.

constitutive equation and it is necessary in order to prevent instabilities related to HWNP. In their work, Chen *et al.* (2013) examines the positivity of the conformation tensor by monitoring the sign of its determinant. If the matrix is initiated definite positive, then the first sign change of any of the eigenvalues will result in a negative determinant. Considering the log-conformation technique, setting Re = 2000, α_G = 0.15 and 0.45, β = 0.25 and 0.75, and varying Wi = 5; 20 and 80, the determinant of conformation tensor $|\boldsymbol{A}|$ is shown in Figure 6. This way, it is possible to notice that the log-conformation formulation preserved $|\boldsymbol{A}|$ always greater than zero, that is, there was never a loss of positivity in this matrix.

According to Hulsen (1988), the positivity of the conformation tensor is ensured if the determinant of this tensor, positive initiate, satisfies $|\boldsymbol{A}| \geq 1$. In fact, in all cases $|\boldsymbol{A}| \approx 1$, confirming the results previously presented for flow stability analysis using log-conformation as a strategy to stabilize the HWNP.

7. CONCLUSIONS

In present paper, the log-conformation formulation for stabilization of the HWNP is presented. Considering the two-dimensional Poiseuille flow of Giesekus viscoelastic fluid, the stability analysis for flows was performed using the Direct Numerical Simulation (DNS) technique and the governing equations are written in a vorticity-velocity formulation.

In order to evaluate the maximum amplification rates, different dimensionless parameter values were tested for Newtonian and non-Newtonian fluid flows, with particular attention to Weissenberg number and the parameter β, which controls the Newtonian contribution of the fluid.

In addition, an analysis of the minimum determinant value of the conformation tensor was carried out for some particular cases, where it was possible to verify that the values obtained are satisfactory, according to the literature, ensuring that the results referring the stability analysis are consistent.

8. ACKNOWLEDGEMENTS

We thank the Coordination for the Training of Higher Education Personnel (CAPES) for the research grant we received during the development of this study.

9. REFERENCES

Afonso, A.M., Pinho, F.T. and Alves, M.A., 2012. “The kernel-conformation constitutive laws”. *Journal of Non-Newtonian Fluid Mechanics*, Vol. 167, pp. 30–37.

Brandi, A.C., Mendonça, M.T. and de Souza, L.F., 2017. “Comparação de DNS e LST para o escoamento de Poiseuille do fluido Oldroyd-B”. In *13º Congresso Ibero-americano de Engenharia Mecânica*. Lisboa, Portugal.

Chen, X., Marschall, H., Schafer, M. and Bothe, D., 2013. “A comparison of stabilisation approaches for finitevolume simulation of viscoelastic fluid flow”. *Journal of Computational Fluid Dynamics*, Vol. 27, p. 229–250.

Dupret, F. and Marchal, J.M., 1986. “Loss of evolution in the flow of viscoelastic fluids”. *Journal Non-Newtonian Fluid Mechanics*, Vol. 20, pp. 143–171.

Fattal, R. and Kupferman, R., 2004. “Constitutive lows for the matrix-logarithm of the conformation tensor”. *Journal of Non-Newtonian Fluid Mechanics*, Vol. 123, pp. 281–285.

Fattal, R. and Kupferman, R., 2005. “Time-dependent simulation of viscoelastic flows at high Weissenberg number using the log-conformation representation”. *Journal of Non-Newtonian Fluid Mechanics*, Vol. 126, pp. 23–37.

Giesekus, H., 1982. “A simple constitutive equation for polymer fluids based on the concept of deformation-dependent tensorial mobility”. *Journal of Non-Newtonian Fluid Mechanics*, Vol. 11, pp. 69–109.

Hulsen, M.A., 1988. “Some properties and analytical expressions for plane flow of leonov and giesekus models”. *Journal Non-Newtonian Fluid Mechanics*, Vol. 30, pp. 85–92.

Martins, F.P., Oishi, C.M., Afonso, A.M. and Alves, M.A., 2015. “A numerical study of the kernel-conformation transformation for transient viscoelastic fluid flows”. *Jornal of Computacional Physics*, Vol. 302, pp. 653–673.

Souza, L.F., Mendonça, M.T. and Medeiros, M.A.F., 2005. “The advantages of using highorder finite differences schemes in laminar-turbulent transition studies”. *International Journal for Numerical Methods Fluids*, Vol. 48, pp. 565–592.

10. RESPONSIBILITY NOTICE